ELSEVIER

Polymer 40 (1999) 4659–4665

polymer

The molecular conformations of polytetrafluoroethylene: forms II and IV

E.S. Clark*

Department of Materials Science and Engineering, The University of Tennessee, Knoxville, TN, 37996-2200, USA

Dedicated to Professor Ronald K. Eby on the occasion of his 70th birthday

Received 18 July 1998; received in revised form 8 February 1999; accepted 8 February 1999

Abstract

The crystal structure of polytetrafluoroethylene, $-(CF_2)_n-$, is unusual in having a number of crystal forms and also possessing substantial molecular motion within the crystal well below the melting point. This article deals with the unusual first-order transition occurring at about 19°C, changing the crystal structure from form II to form I. This article also updates current literature on the crystal structures of these two forms. X-ray and electron diffraction data from forms II and IV are interpreted as helical structures. Form II is defined mathematically as a non-commensurable helix close to a 13/6 conformation of six turns per 13 (CF_2) groups. Form IV is interpreted as a commensurable 15/7 helix which is consistent with space group $P3_1$. Fiber diffraction patterns of these forms are described in detail.

Keywords: Polytetrafluoroethylene; First-order transition; Non-commensurable helix

1. Introduction

The crystal structure of polytetrafluoroethylene (PTFE), $-(CF_2)_n-$, is unusual in having a number of crystal forms and also possessing substantial molecular motion within the crystal well below the melting point. This article deals with the unusual first-order transition occurring at about 19°C [1]. In particular, this article updates a primary literature reference to the transition which the author presented in 1956 [2]. In this article, the first-order transition at 19°C between forms II and IV (see Fig. 1) was interpreted as an untwisting in the helical conformation of the molecule from a 13/6 conformation to a 15/7 conformation. (The relationship between the nomenclature of screw axes and helical conformations is given in the Appendix.) Additional research has shown that the conformation in form II is not a commensurable helix as reported in the earlier article, i.e. the conformation cannot be expressed as a ratio of simple whole numbers. However, an argument will be presented that the form IV may possess a commensurable 15/7 conformation.

2. The helical conformation and X-ray fiber patterns

2.1. The commensurable helix

Fig. 2 shows the molecular conformation of form II as presented in the 1956 article [2]. The conformation is equivalent to a planar polyethylene type zig-zag which is given a 180° twist in 13 (CF_2) motifs. This is a 13/6 helix, i.e. the atoms are evenly spaced along a helix having six turns per 13 atoms to form the repeat unit. The structure is defined in terms of three helices—one for the carbon and one for each fluorine. For a non-commensurable helix, i.e. one which cannot be expressed as the ratio of simple whole numbers, the conformation may be expressed as the ratio of the pitch, P, to the axial spacing, s, of the atoms on the helix as illustrated in Fig. 2 for a helix of 13 units (u) per six turns (t). Thus, $u/t = P/s = 13/6 = 2.1667$ (CF_2) motifs per turn. X-ray patterns of PTFE fiber are shown in Fig. 3. These were made with a Unicam 60 mm diameter cylindrical camera with Cu (Ni) radiation. A distinctive feature of helical conformations such as these is the distribution of intensity among the layer lines. In particular, the twisted zig-zag conformation is characterized by two intense layer lines displaced by about $\zeta = 0.4\,\text{Å}^{-1}$ (axial reciprocal lattice direction); these are layer lines six and seven for form II, and seven and eight for form IV as shown in Fig. 3.

A mathematical treatment of the commensurable helical conformations has been presented by Clark et al. [3]. This

* Tel.: + 1-423-974-4410.
E-mail address: eclark@usit.net (E.S. Clark)

0032-3861/99/$ - see front matter
PII: S0032-3861(99)00109-3

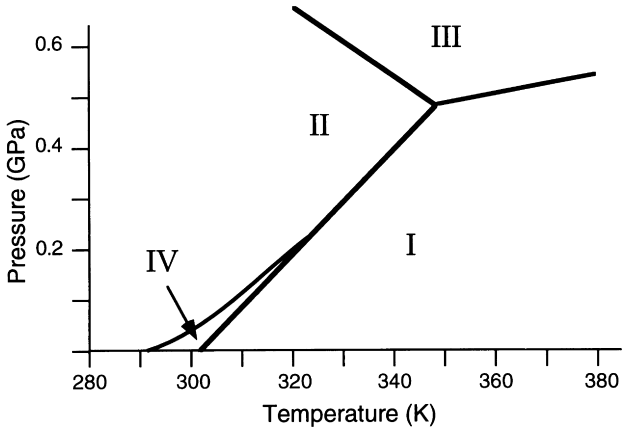

Fig. 1. Phase diagram of polytetraflouroethylene[12].

approach is based on the method of Cochran et al. [4] in terms of atoms regularly spaced along a helix as illustrated in Fig. 2. If the helix is commensurable with t turns in u units, there will be a repeat distance, c, and

$$r^* = u^*/t^* = P^*/s^*; \qquad c = u^*s^* = t^*P^*, \tag{1}$$

where the asterisk indicates commensurability. As shown by Cochran et al. [4], the fiber pattern can be modeled using Bessel functions governing the intensity distribution in each layer line according to the selection rule:

$$\ell = t^*n + u^*m, \tag{2}$$

where ℓ is the layer line number, n, the order of Bessel function and m, any integer. With the identity period, c, associated with commensurability, the layer lines will be evenly spaced along z in reciprocal space on integer layer lines ℓ

$$\zeta_\ell = \frac{\ell}{c} = \frac{\ell}{u^*s} \tag{3}$$

with uniform spacing between the layer lines

$$\Delta\zeta = \frac{1}{t^*P^*} = \frac{1}{u^*s}. \tag{4}$$

Within the layer lines of a fiber pattern, the distribution of intensity for a commensurable helix is approximated by the cylindrically symmetrical transform of a helical conformation with atoms at cylindrical coordinates, (r_j, ϕ_j, z_j) for each atom of the asymmetric unit (CF_2) repeating along the helix. The cylindrically averaged intensity function has been given in a convenient form by Davies and Rich [5]:

$$F^2_{\bar{\psi}}(R, \frac{\ell}{c}) = \sum_n (A_n^2 + B_n^2), \tag{5}$$

where

$$A_n = \sum_j f_j \mathrm{J}_n(2\pi r_j R)\cos\left[n\left(\frac{\pi}{2} - \phi_j\right) - \frac{2\pi\ell}{c} z_j\right],$$

$$B_n = \sum_j f_j \mathrm{J}_n(2\pi r_j R)\sin\left[n\left(\frac{\pi}{2} - \phi_j\right) - \frac{2\pi\ell}{c} z_j\right].$$

The solutions of the selection rule, Eq. (2) for the 13/6 and 15/7 conformations are shown in Fig. 4. An illustration of the intensity distribution for the 13/6 conformation is shown in Fig. 5, with the contours indicating relative intensity distribution in the layer lines. In this conformation, the sixth and the seventh layers, being governed by a first-order Bessel function are of dominant intensity. For the 15/7 conformation, these are the seventh and eighth layers. As a matter of experience, only layer lines with Bessel functions less than about five will be observed on a fiber pattern. The relationship among these features may be seen for the 13/6 conformation by comparing Figs. 2–5. It may be noted that the separation of these intense layer lines for the 15/7 conformation is less than that for the 13/6 conformation. For an untwisted planar zig-zag, the separation is zero; the two layer lines overlap into a single layer line.

2.2. The non-commensurable helix

In the case of a non-commensurable helical conformation, there is no translational identity, i.e. the repeat distance

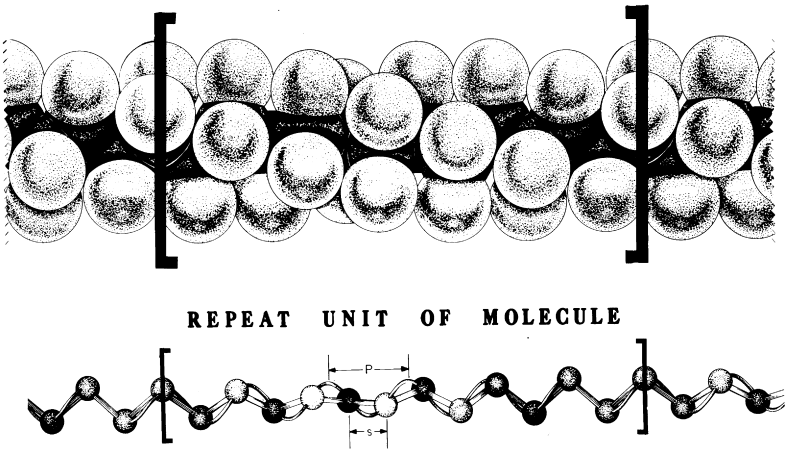

Fig. 2. Repeat unit for a 13/6 conformation and the helical definition of the carbon backbone.

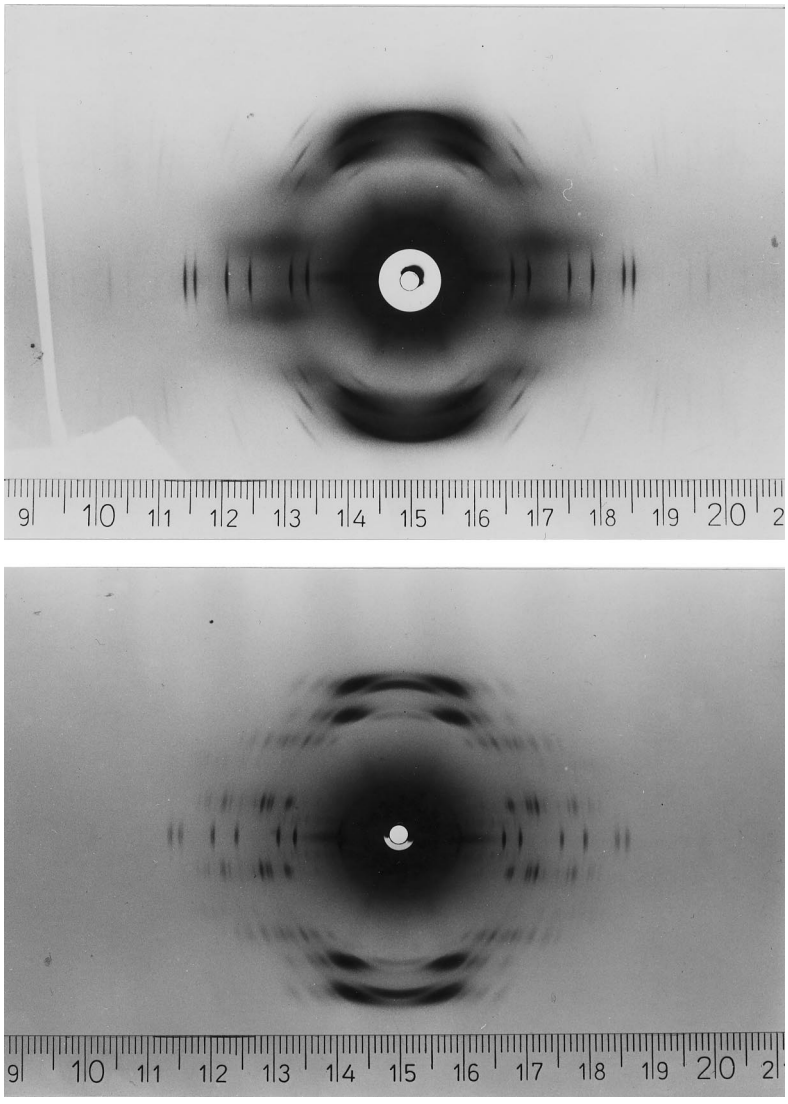

Fig. 3. X-ray fiber patterns of PTFE fiber in form II (below) and form IV (above).

c lacks meaning. However, the fiber pattern will appear similar to that for a commensurable helix. In this case, the conformation is expressed simply by the ratio r:

$$r = \frac{u}{t}. \tag{6}$$

The non-commensurable helix is treated in terms of a modification of a close commensurable helix. Thus, 13/6 = $r = 2.167$. It will be shown that the correct value for form II is $r = 2.159$. Thus the fiber pattern of form II is treated as a modification of 13/6. The ratio P/s is likewise not the ratio of simple numbers, and

$$\zeta_\ell = \frac{n}{P} + \frac{m}{s}. \tag{7}$$

The expressions developed for evaluating the conformation of the non-commensurable helix require accurate evaluations of the layer line heights, ζ, and the assumption that the atom spacing, s, is an invariant. In the case of PTFE, the axial spacing, s, is nearly a constant at 1.300 Å. In this procedure, the layer line heights for the commensurable helix are calculated by Eq. (7). The actual measured heights are compared with the calculated heights for the commensurable helix (13/6) as displacements of the measured layer line height from that calculated as

$$\Delta\zeta = \frac{\ell}{u^*s} - \frac{n}{rs} - \frac{m}{s}. \tag{8}$$

The variables ℓ and u^* are those from the commensurable helix with s invariant.

3. The helical conformation of polytetrafluoroethylene form II

Fibrous crystals of essentially 100% crystallinity were produced by the author using an unusual procedure by electron diffraction in the year 1959 at the DuPont Experimental

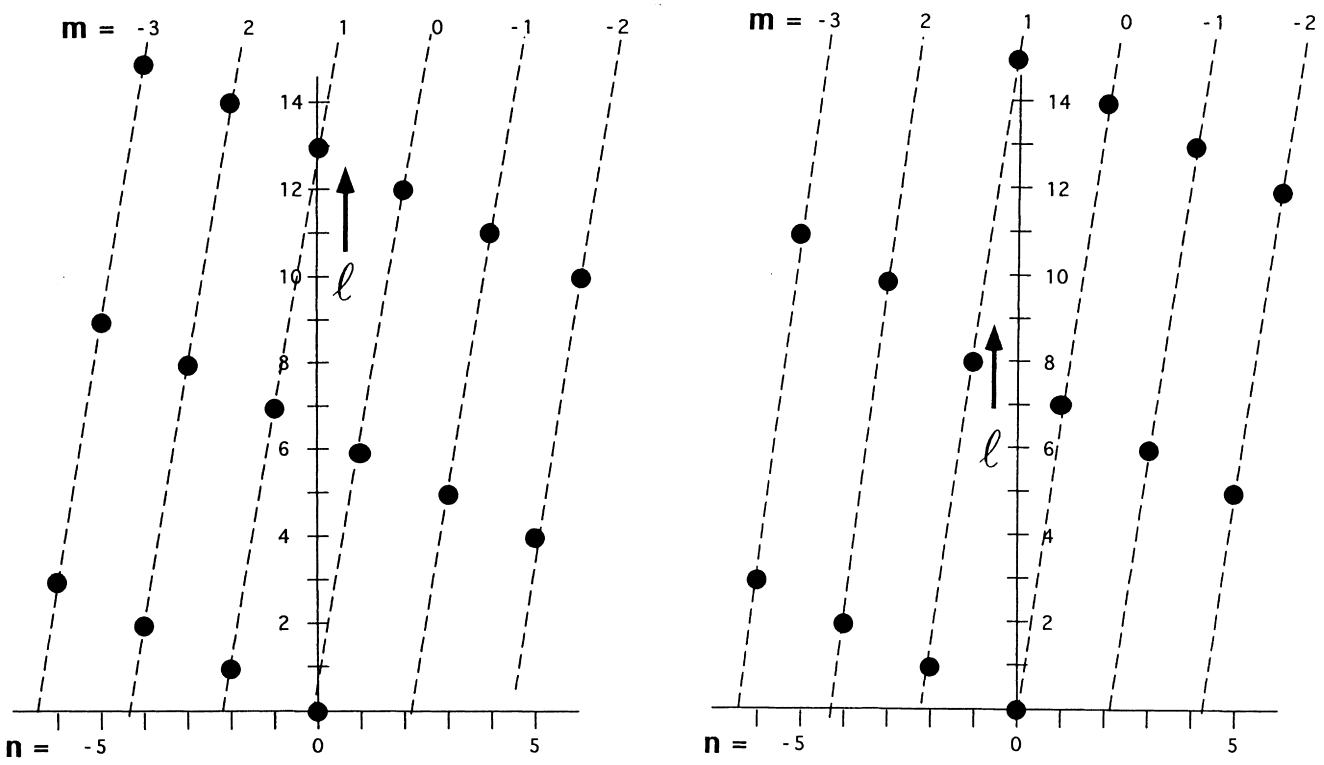

Fig. 4. Solutions of the selection rule for the 13/6 conformation (left) and the 15/7 conformation (right).

Station. The procedure is described in Ref. [3]. Examples of the patterns obtained are shown in Figs. 6 and 7. The distinctive distribution of layer line intensity is clearly evident, in agreement with that calculated in Fig. 5. Of special interest in Fig. 7 are the sharp meridional spots on the 13th and 26th layers (very top of pattern). These are in agreement with a zero-order Bessel function distribution from Fig. 4. Similar electron diffraction patterns were recorded by Kimmig et al. using a different sample preparation technique. Several electron diffraction patterns similar to Figs. 6 and 7 were measured with great care (by J. Weeks) making corrections for the small geometric distortion of flat plate photography and slight tilts of the fiber axis from normality to the electron beam. Details of this analysis are in Ref. [3]. Using the mathematical approach of Eq. (8), the analysis of three patterns gave the results shown in Table 1.

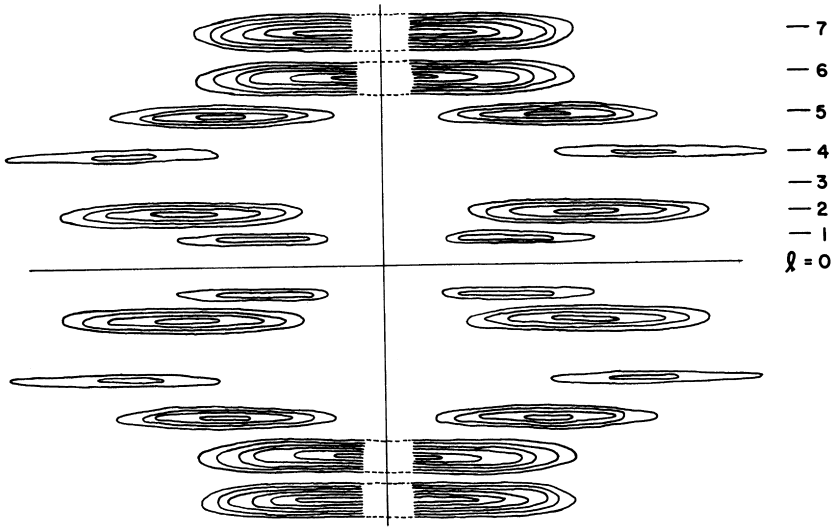

Fig. 5. Calculated fiber pattern for 13/6 conformation showing relative intensities as contours.

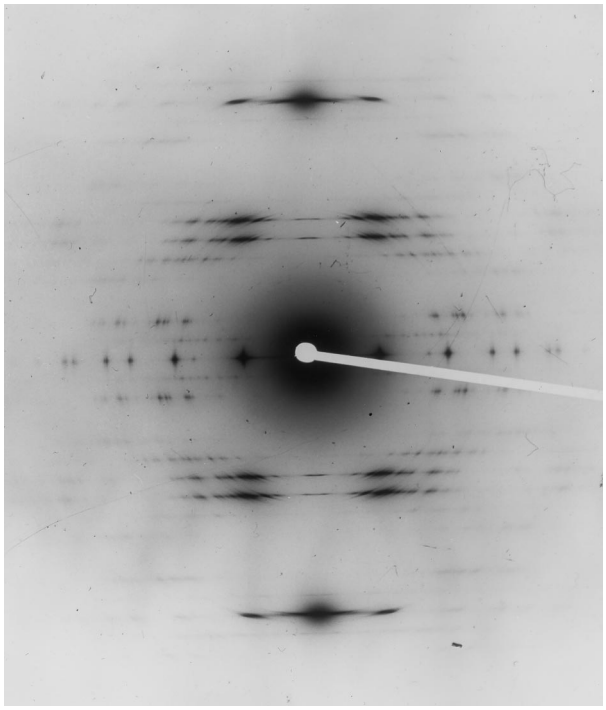

Fig. 6. Electron fiber diffraction pattern of form II showing similarity with calculated pattern of Fig. 5.

From a review of the measurements and the quality of the patterns, the best value for the molecular conformation in form II is given in Table 2.

It is easily seen that the specification of 948 units per 439 turns or a conventional repeat unit of 1232 Å is meaningless. The conformation may be visualized as 13/6 helix as a reasonable approximation. The differences among the specifications for forms II and IV are illustrated in Fig. 8.

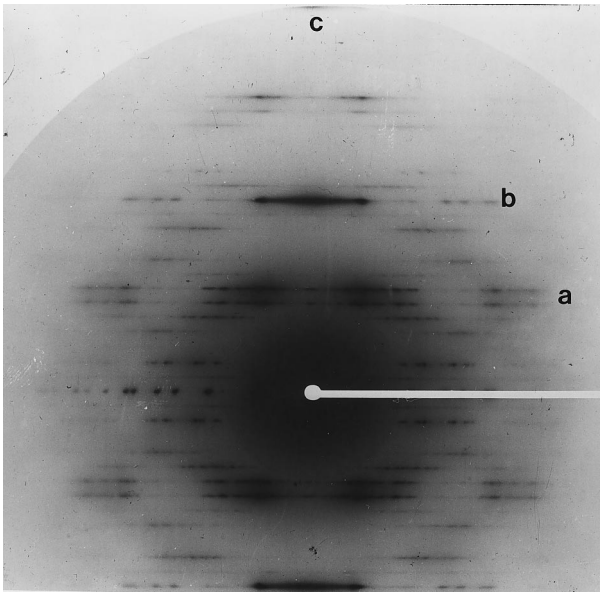

Fig. 7. Electron fiber diffraction pattern of form II showing sixth and seventh orders (a), 13th order (b) and 26th order (c).

Table 1
Electron diffraction results

Plate	s (axial) (Å)	$R = u/t$
A	1.288	2.1613
B	1.299	2.1597
C	1.298	2.1592

4. The helical conformation of polytetrafluoroethylene form IV

The X-ray fiber pattern of form IV is shown in Fig. 3; electron diffraction patterns are shown in Fig. 9 for different exposures. The patterns are distinctive in showing a mixture of both sharp spots and diffuse streaks, as discussed in detail by Clark and Muus [6]. This combination implies that the helical chains undergo small angular displacements about their long axis. From the nuclear magnetic resonance experiments by Hyndman and Origlio [7] on the same fiber used for the X-ray experiments, it was concluded that the chains are disordered by torsional oscillation about the long axis. An interpretation of this type of disorder from electron diffraction measurements is given in Ref. [8]. As shown by Clark and Muus, for small angular oscillations, the intensities of the Bragg reflections in a layer line decrease with increasing order of the controlling Bessel function, according to the selection rule illustrated in Fig. 4. (As the intensity of the Bragg reflection decreases, the layer line continuum streak correspondingly increases). This type of librational disorder involves NO displacement of the chains along the long axis. This requires that Bragg reflections in layer lines controlled by zero-order Bessel functions remain unaffected. Therefore reflections on the equator and 15th layer should remain sharp and unaffected while the layers in-between show decreasing Bragg intensity and increasing streaking. Fig. 10 is a fiber pattern from the same 60-cm cylindrical camera with the fiber perpendicular to the rotation axis of the camera and tilted to the incident beam to enhance the intensity of reflections near 1.3 Å (the 15th layer). The sharp reflections on the zero layer and the 15th layer (above the 16.7 scale marker) confirm the interpretation. The small peak below the intense 0,0,15 is a Kβ reflection. The sharpness of the 1,0,15 reflection at a d-spacing of less than 1.3 Å requires very high longitudinal order. This interpretation is strongly supported by the electron diffraction pattern of Fig. 9. The nature of the sharp reflections in Fig. 9 does not permit an analysis of the conformation with the accuracy used for form II. However, accurate data was obtained from X-ray diffraction. A special

Table 2
Molecular conformation of form II

	P/s	u/t	c (repeat) (Å)
Old	2.167	13/6	16.9
Revised	2.159	948/439	1232

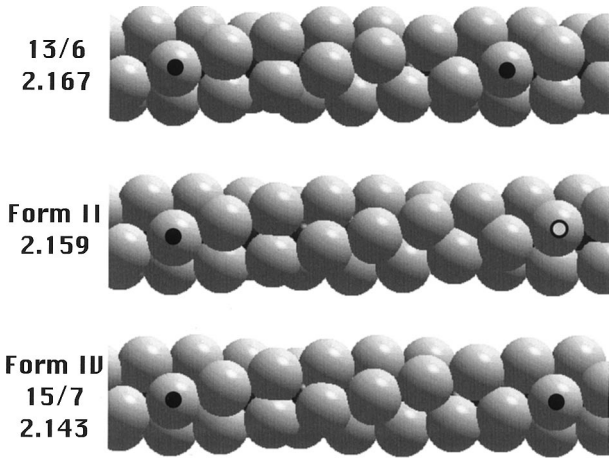

Fig. 8. Illustrations of PTFE conformations. (Constructed with MacMolecule ver. 1.7).

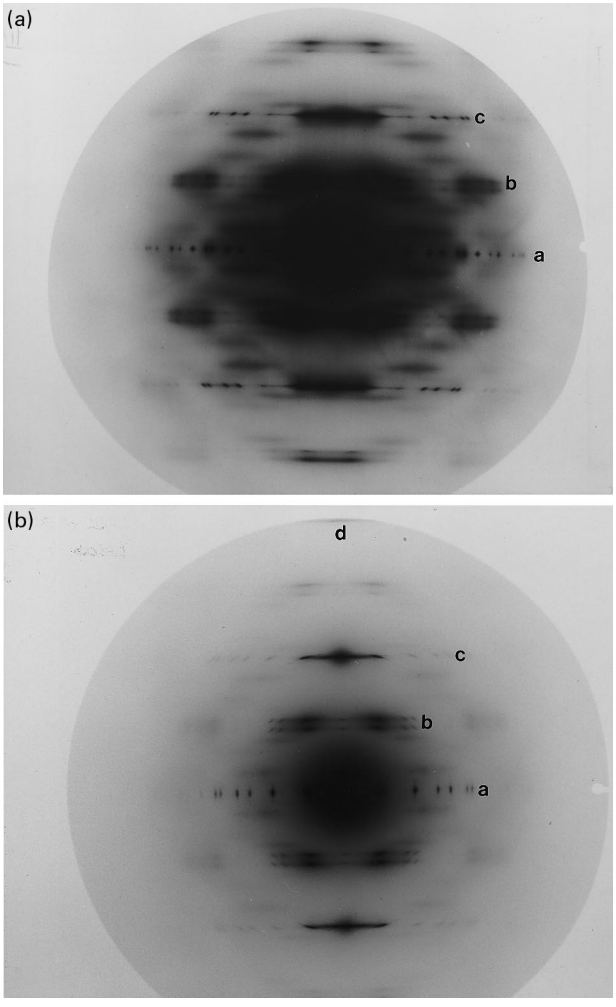

Fig. 9. Electron fiber diffraction patterns of form IV showing equator (a), seventh and eighth layers (b), 15th layer (c) and 30th layer (d).

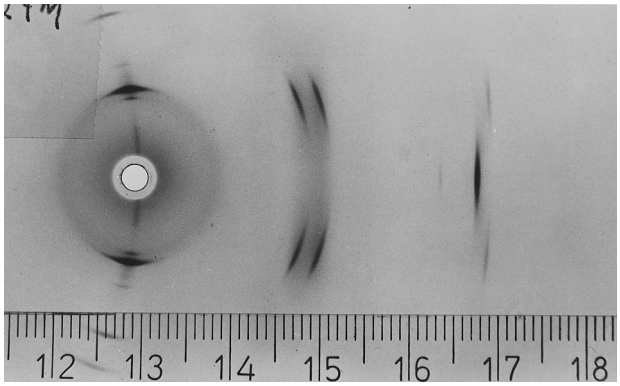

Fig. 10. Tilted X-ray fiber pattern of form IV showing 15th layer Bragg reflections.

sample was prepared (at the DuPont Experimental Station) of a mixture of PTFE powder and spectroscopically pure KCl powder. This mixture was compressed and carefully sintered for maximum development of crystallinity. X-ray data were recorded with a Philips Norelco diffractometer and scintillation counter. The observed reflections for 110, 200, 107 and 108 were measured in addition to the KCl reflections. The PTFE reflections were corrected using differences from calculated KCl peaks using data from Glover [9]. These data from form IV and results are shown in Fig. 11. Within the limits of error, the conformation corresponds to that given in Table 3. A comparison of this conformation with that of form II is illustrated in Fig. 8.

From the relationships presented in the Appendix, the conformation 15/7 possesses the crystallographic symmetry 3_1. Therefore, the proposal is offered that at 19°C, transition is characterized by the onset of molecular oscillations, perhaps associated with chain reversals as discussed by

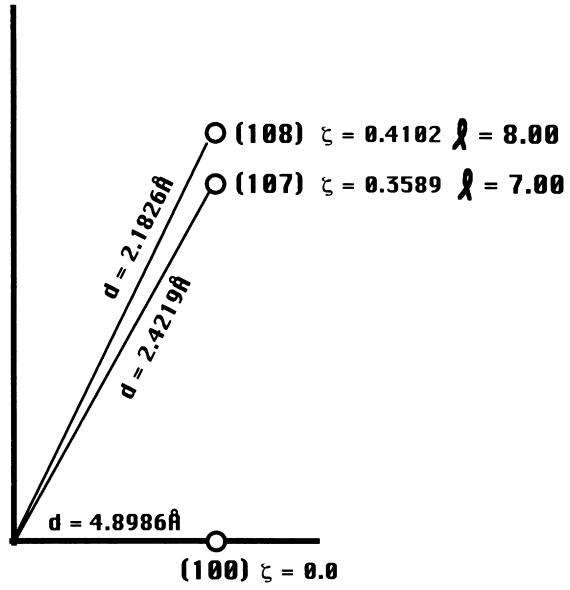

Fig. 11. Layer line data and calculations for form IV from X-ray powder pattern.

Table 3
Molecular conformation of form IV

P/*s*	*u*/*t*	*c* (repeat) (Å)
2.143	15/7	19.5

Table 4
Lateral arrangement of chain axes

	$a' = b'$ (Å)	γ' (°)	Density (kg/m^3) (calculated)
Form II (0°C)	5.59	119.3	2344
Form IV (25°C)	5.66	120	2302

Kimmeg et al. [8]. As the chain untwists from non-crystallographic symmetry, it reaches the symmetry of 3_1 corresponding to the space group $P3_1$ producing a small lowering of packing energy. This causes the conformation to remain in this 15/7 conformation until increasing energy causes additional untwisting to continue at the 30°C transition. This may be an explanation for the very small temperature range of form IV.

5. The lateral packing of the chains

For completeness, some comments should be made on the lateral packing of the chains. As shown in Fig. 8, all forms of PTFE are nearly cylindrical in shape and all forms pack with nearly hexagonal packing. The lateral packing parameters for forms II and IV are given in Table 4. The constants a', b' and γ' refer to the placement of the chain axes. For a discussion of g1, the complex unit cell of form II, see Ref. [10].

Appendix A. Symmetry notation in helical conformations [11]

Two notations are employed for defining atoms that are regularly spaced along a helical net. These two systems may be termed translational notation (*u*/*t*) for *u* atoms spaced along *t* turns of the helix and rotational notation, u_g which for crystallographic (three-dimensional) symmetry is the screw axis notation. The parameters *u*, *t* and *g* must be positive integers. In both systems of notation, the helical structure is generated by repeated operation of rotation through angle Θ accompanied by a translation, *Z*, along the helical axis.

A.1. Rotational notation

The operators Θ and *Z* are:

$$\Theta = \frac{2\pi}{u} \qquad \text{and} \qquad Z = \frac{g}{u}c = gs,$$

where *c* is the crystallographic repeat distance (if present) and *s*, the axial spacing between adjacent units. This notation is used for structures with crystallographic symmetry, e.g. 2_1, 4_3, 3_1.

A.2. Translational notation

The operators Θ and *Z* are:

$$\Theta = \frac{2\pi s}{P} = 2\pi\frac{t}{u} \qquad \text{and} \qquad Z = s = \frac{c}{u},$$

where *P* is the pitch of the helix. This notation is commonly used for polymeric chains which may not be treated by space group symmetry, e.g. PTFE, 13/6; alpha helix, 18/5.

The relationship between the two notations is:

$$gt = \varepsilon u + 1,$$

where ε is the lowest positive integer which can solve the equation. Thus, for 15/7 conformation, $\varepsilon = 6$ corresponding to a 15_{13} screw axis. Note that 15_{13} and 15_2 are the left- and right-handed versions of the same helical conformation. The condition for the number pair appears to be the same, i.e. u_g and *u*/*t* is:

$$g^2 = t^2 = \varepsilon u + 1.$$

References

[1] Sperati CA, Starkweather Jr. HW. Fortschr HochpolymForsch 1961;2:465.
[2] Pierce RHH Jr, Clark ES, Whitney JF, Bryant WMD. Abstract of Papers, 130th Meeting of the American Chemical Society, September, 1956, 9S.
[3] Clark ES, Weeks JJ, Eby RK. ACS Symposium Series 1980;141:183.
[4] Cochran W, Crick FHC, Vand V. Acta Crystallogr 1952;5:581.
[5] Davies DR, Rich A. Acta Crystallogr 1959;12:97.
[6] Clark ES, Muus LT. Z Krist 1962;117:119.
[7] Hyndman D, Origlio GF. J Appl Phys 1960;31:1849.
[8] Kimmeg M, Strobl G, Stühn B. Macromolecules 1994;27:2481.
[9] Glover Z. Physik 1954;138:224.
[10] Weeks JJ, Clark ES, Eby RK. Polymer 1981;22:1480.
[11] Clark ES, Muus LT, Paper presented to the American Crystallographic Association Meeting, Bozemann MT, 1964.
[12] Eby RK, Clark ES, Farmer BL, Piermarini GJ, Block S. Polymer 1990;31:2227.